



Dithizone-Immobilized Nickel Slag for Removing Lead (II) Ion

W. M. Pratama^{1*}, N. H. Aprilita¹, M. Mudasir¹

¹ Department of Chemistry, Faculty of Mathematics and Natural Sciences, University of Gadjah Mada
Sekip Utara, Yogyakarta 55281, Indonesia

* wisnupratama165@gmail.com

Received 26 Sept 2022,
Revised 09 Oct 2022,
Accepted 10 Oct 2022

Keywords

- ✓ dithizone
- ✓ Pb (II),
- ✓ nickel slag,
- ✓ immobilization,
- ✓ adsorption.

wisnupratama165@gmail.com;

Abstract

The batch approach was utilized for Pb (II) ion adsorption onto dithizone-immobilized nickel slag (DNS). The investigation was initiated by activating nickel slag (NS) and then immobilizing dithizone on active nickel slag (ANS). Several adsorption factors, including pH, adsorbent dose, interaction time, and initial lead concentration, were examined. XRD and FT-IR tests reveal that dithizone has been satisfactorily immobilized on nickel slag that has been activated (ANS). The optimal conditions for Pb (II) adsorption are pH 6, 20 mg mass, 60 minutes, and a concentration of 80 mg L⁻¹ of lead. The pseudo-second order kinetic model and the Langmuir isotherm are utilized to characterize lead adsorption. DNS has superior capacity absorption compared to ANS.

1. Introduction

As an industrial byproduct, numerous hazardous heavy metals have been released into the environment [1]. Lead (Pb) is among the harmful heavy metals. The accumulation of lead has issues for environmental and human health. The chronic effects of lead in the human body are characterized by several diseases such as disruption of hemoglobin biosynthesis, renal damage, hypertension, children with brain injury, and diminished learning ability [2,3]. Glass production, metal plating, battery production, paint, porcelain, and acid rock drainage are the primary environmental causes of lead pollution [4].

Several procedures for removing heavy metals have been implemented, including reverse osmosis, phytoextraction, precipitation, ion exchanges, ultrafiltration, and also electrodialysis. Nevertheless, these strategies are costly and require the use of cutting-edge technology [5]. Adsorption is the ideal technique for reducing lead due to its good efficiency in the purification process, its simplicity in experimental setup, and the availability of several affordable adsorbents [6,7]. Recently, adsorption methods for heavy metal removal have been reported [5,8–10].

Nickel slag (NS) is a solid result of melting nickel-iron alloy. SiO₂, MgO, CaO, Al₂O₃, P₂O₅, and FeO are among the chemical constituents of NS [11,12]. The main composition of nickel slag differs depending on the melting method and ore source. In recent years, slag has been utilized in cement mixtures, concrete mixtures, and road building [13–15]. In addition, slag has been described as an inexpensive heavy metal adsorbent [15–19]. However, natural slag has a low adsorption capacity and

selectivity as an adsorbent. Before it can be utilized as an adsorbent, its capacity and selectivity should be enhanced. The addition of a chelating agent and ligands to its surface is one way to increase its adsorption capacity and selectivity. As a result of the existence of active groups including NH, SH, and N, dithizone has been recognized as an effective heavy metal chelating agent [10]. Loading dithizone as a chelating agent on adsorbents like zeolite, bentonite, bottom ash, and silica gel can enhance their adsorption capacity [5,10,20,21]. Therefore, this research was conducted to synthesize nickel slag immobilized with dithizone (DNS). In contrast, the impact of operating factors such as interaction time, pH, initial lead, and slag dose on lead (II) adsorption efficiency is studied. In addition, the kinetics and isotherm model of adsorption are determined.

2. Methodology

2.1 Materials and instruments

Nickel Slag from ANTAM Ltd., Pomala, Sulawesi, Indonesia. Dithizone (Merck), HCl 37% (Merck), ethanol (Merck), double distilled water, lead nitrate ($\text{Pb}(\text{NO}_3)_2$) (Merck), toluene (Merck), the buffer acid used is made from trisodium citrate dihydrate ($\text{C}_6\text{H}_5\text{Na}_3\text{O}_7 \cdot 2\text{H}_2\text{O}$) (Merck) and citric acid ($\text{C}_6\text{H}_8\text{O}_7 \cdot \text{H}_2\text{O}$) (Merck), buffers base is made from trisodium phosphate dodecahydrate ($\text{Na}_3\text{PO}_4 \cdot 12\text{H}_2\text{O}$) (Merck) and sodium dihydrogen phosphate monohydrate ($\text{NaH}_2\text{P}_2\text{O}_7 \cdot \text{H}_2\text{O}$) (Merck). XRF (PAN analytical-Type mini pal 4), AAS (Perkin Elmer 3110), FTIR spectrophotometer (Shimadzu-IR Prestige-21 and 8201 PC), XRD (Rigaku Miniflex-600), magnetic stirrer, heater, reflux set, analytical balance (Mettler AE 200), Mettler Toledo pH meter, 250 mesh sieve, porcelain, Whatman 42 filter paper.

2.2 Synthesis of dithizone-immobilized nickel slag (DNS)

This experiment employs a technique similar to those previously described for bentonite [5]. To begin with, crushing the nickel slag and sieving it at 250 mesh. In addition, NS was analyzed by XRF to obtain information about the chemical components of nickel slag. Prior to immobilization, nickel slag was activated by the reflux method using 6 M HCl for four hours at a temperature of 110 °C. The pH of the activated nickel slag (ANS) was neutralized by washing it with distilled water. Next, the immobilization procedure was carried out by stirring dithizone (1 g) in toluene and ANS (4 g) at 50 °C for four hours. Before being cleaned with toluene, ethanol, and distillate water, the DNS was filtered and washed until no dithizone remained. Then, the DNS was then dried for 6 hours at 50 °C. The ANS and the DNS were characterized by XRD and FTIR before being used in investigations involving adsorption.

2.3 Study of adsorption Pb (II)

A batch process was utilized for lead (II) adsorption. To investigate the impact of solution pH, 100 mg of DNS and ANS were reacted for 120 minutes with 10 mg L^{-1} of 10 mL of Pb (II) in separate beaker glasses. Using buffer solutions, the acidity of the solution was adjusted from 3-8. Also determined was the optimal mass adsorbent by altering 10-400 mg of slag doses at the optimal pH. The contact time was determined to be 15-180 minutes at the optimal pH and dose. Using kinetic models, the obtained data was analyzed. The initial Pb (II) concentration on DNS and ANS determined the isothermal adsorption. Initial lead (II) values of 10, 30, 50, 80, and 100 mg L^{-1} were examined. Using the Freundlich and Langmuir adsorption isotherm models, the outcomes were analyzed. Using an AAS spectrophotometer, the Pb (II) ion was measured.

3. Results and Discussion

3.1 The main chemical compound of nickel slag (NS)

The primary chemical constituent of NS from ANTAM Ltd was analyzed using XRF. Table 1 displays the primary chemical components of NS. According to table 1, the principal components of ANTAM's NS are SiO₂, Fe₂O₄, MgO, Al₂O₃, and CaO. In NS, silica becomes the most abundant element. The main component of NS is similar to the previous report [11,22,23]. Table 1 indicates that the activation of NS with HCl reduced various contaminants in NS and raised the SiO₂ mass percentage. The activation of nickel slag is also to convert SiO₂ groups on the slag surface into more active silanol groups.

Table 1. The chemical components of NS and ANS from Antam Ltd.

No	Compounds	Contents (%)	
		NS	ANS
1	SiO ₂	47.60	60.10
2	Fe ₂ O ₃	31.00	23.20
3	MgO	12.30	9.55
4	Al ₂ O ₃	2.65	1.88
5	CaO	2.18	1.71

3.2 XRD Spectra

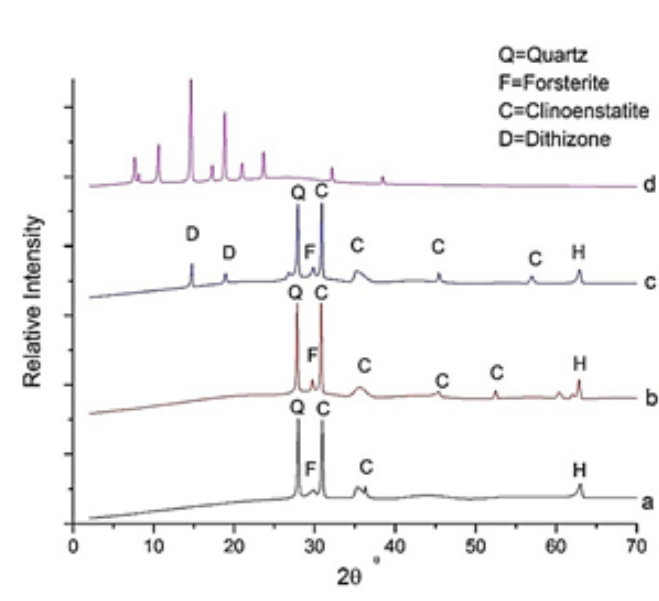


Figure 1. XRD spectra of NS (a), ANS (b), DNS (c), dithizone (d)

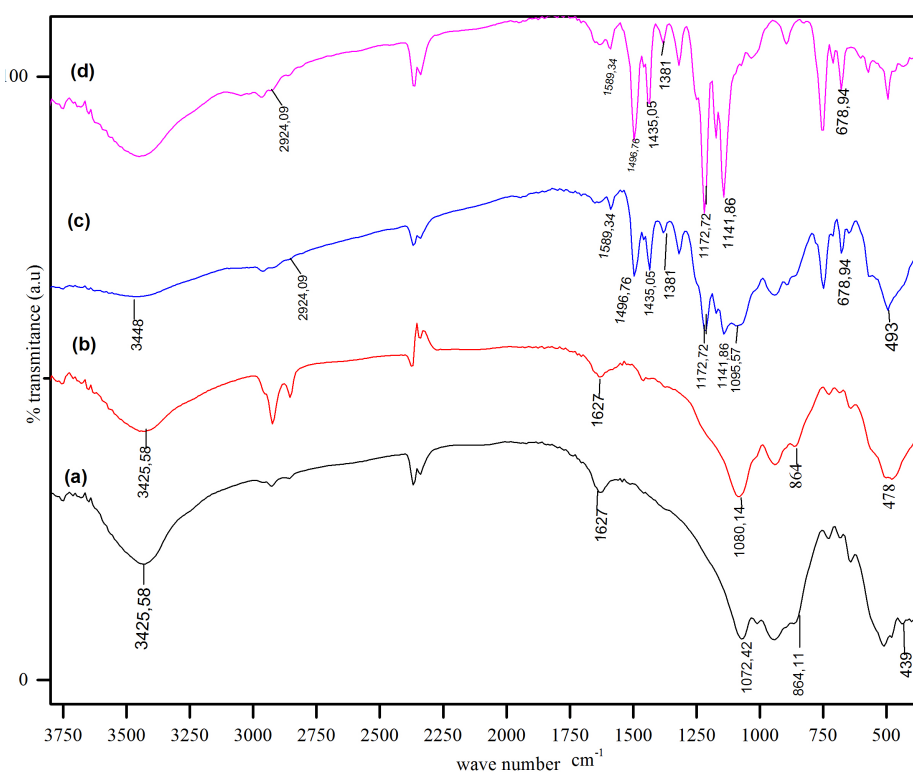
XRD was used to characterize the acquired DNS in order to substantiate that dithizone was effectively immobilized on the surface of ANS. Figure 1 demonstrates the distinct XRD peaks of NS (a), ANS (b), DNS (c), and pure dithizone (d). According to the JCPDS database [24], the peaks of specific minerals in ANS are as follows: quartz at 27.93, forsterite at 29.85, clinoenstatite at 30.88, 35.14, 45.39, and 56.94, and hematite at 62.85. Furthermore, the XRD pattern reveals distinctive dithizone peaks at 14.75 and 18.93 (figure 1-c). The existence of dithizone peaks on DNS implies that dithizone has been immobilized successfully on the ANS. Table 2 presents an overview of the comprehensive examination of the DNS XRD spectrum.

Table 2. XRD pattern interpretation for DNS

2θ	d	I	Interpretation
14.75	6.00	28.91	Dithizone
18.93	4.68	11.63	Dithizone
27.93	3.19	94.92	Quartz
29.85	2.99	12.50	Forsterite
30.88	2.89	100.03	Clinoenstatite
35.14	2.55	13.76	Clinoenstatite
62.85	1.48	19.17	Hematite

3.3 FTIR Characterization

Figure 2 shows from top to down the IR spectra of free dithizone, dithizone-immobilized nickel slag (DNS), activated nickel slag (ANS), and natural nickel slag (NS), respectively. The IR spectra reveal that the DNS adsorbent has multiple characteristic peaks at 493, 1589, 894, 1095, and 3448 cm^{-1} . At 493 cm^{-1} , the wavenumber directly correlates to the Si-O-Si bending. Due to the bending of H-O-H, a wavenumber of 1589 cm^{-1} is observed. The stretching bond of Si-O and Al-O is linked with wavenumber 894 cm^{-1} . Peak 1095 cm^{-1} belongs to the expansion of Si-O from the Si-O-Al and Si-O-Si groups. Stretching of the -OH group accounts for the peak at 3448 cm^{-1} . The dithizone peaks appear in the FTIR spectrum of DNS at 678, 1141, 1172, 1381, 1435, 1496, and 1501 cm^{-1} .

**Figure 2.** IR of (a) NS, (b) ANS, (c) DNS, (d) dithizone

The maximum at wavenumber 678 cm^{-1} is due to aromatic C-H bending. C-S group vibrations account for the peaks at 1141 and 1172 cm^{-1} . Peak 1381 cm^{-1} is connected with the stretching bond of C-N dithizone, whereas peak 1435 cm^{-1} is confirmed to the vibration of the N=N bond. The C=C aromatic bonds are responsible for the peak at 1496 cm^{-1} . Peak 1589 cm^{-1} is associated with the N-H bending. In table 3, a full analysis of DNS's FTIR characterization is provided. According to the data,

the presence of dithizone in DNS implies that dithizone has been loaded well on the ANS surface. This conclusion is validated by XRD pattern and IR characterization data.

Table 3. The interpretation of the FTIR of DNS

Wavenumber (cm ⁻¹)	Interpretation
493	Si-O-Si deflection
1589	Bending of H-O-H
894	Stretching the symmetry of Al-O and Si-O
1095	Si-O stretching from Si-O-Si and Si-O-Al
3448	Stretching of OH
678	Bending of aromatic C-H
1141 & 1172	Vibration of C=S
1381	Stretching of C-N dithizone
1435	Vibration of N=N bonding
1496	Stretching of aromatic C=C
1589	Bending of N-H

3.4 The Effect of pH solution

The speciation of heavy metal ions in solution and the active site of the adsorbent determine the adsorption of Pb (II) on the ANS and DNS surfaces. The pH modifies the speciation of heavy metal ions as well as the active site of an adsorbent. The impact of the pH solution on the lead (II) adsorption is displayed in figure 3. The graph represents that the adsorption of lead (II) ion by DNS and ANS hits its maximum at pH 6 with capacities of 0.202 mg g⁻¹ and 0.0686 mg g⁻¹, correspondingly. This proves are able to be recognized that the adsorption of Pb (II) climbs with pH until a maximum value is attained, and then declines with pH. Below a pH of 6, acidic active sites become protonated and acquire a partially positive charge.

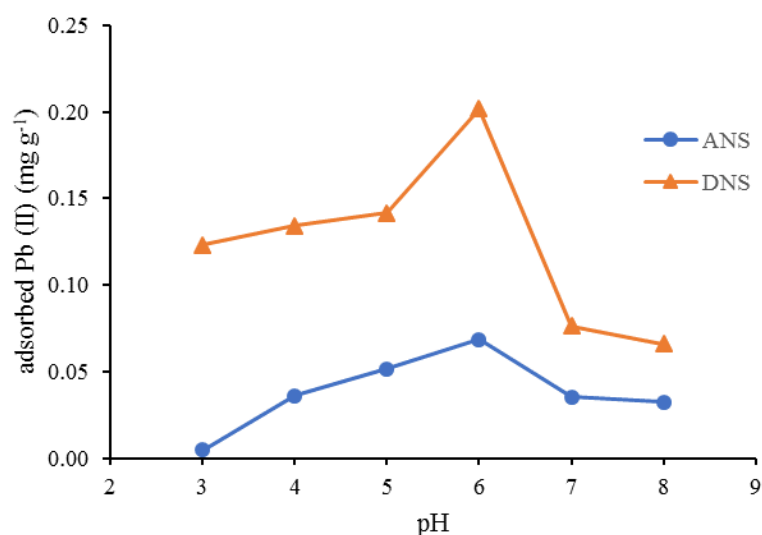


Figure 3. The role of solution pH on the adsorption

The H⁺ concentration is extremely high at low pH, therefore it will compete with Pb²⁺ in the adsorption process. It is obvious that a lower pH solution results in less lead absorption. Once the optimal pH has been obtained, the adsorption of lead reduces as the pH of the solution enhances. The vastly higher the pH value, the greater the amount of OH⁻ ions present. The presence of hydroxide

ion will react with some Pb^{2+} ions to create $Pb(OH)^+$ precipitate that declines the number of lead adsorbed. Based on figure 3, the adsorption capacity of DNS is greater than that of ANS. It is believed that the enhanced contributions of dithizone's active sites, which include N, NH, and -SH groups, are responsible for DNS's enhanced lead ion absorption performance. Citing the Hard Soft Acids and Bases theory (HSAB) of Pearson [25], Pb (II) is a boundary acid that can interact with boundary bases. Active dithizone groups are intermediary bases.

3.5 Implications of slag mass

The influence of slag mass on the adsorption of Pb (II) ion is illustrated in Figure 4. It is clear that the optimal mass for both adsorbents in terms of the effect of ANS and DNS mass on lead (II) adsorption is 0.2 g. After achieving the optimal condition, the amount of lead adsorbed will gradually decrease. Adsorption is predicted to enhance the slag surface area and the number of available adsorption sites as adsorbent mass increases. The equilibrium absorption of lead ion does not rise considerably with increasing adsorbent mass at higher adsorbent dosages. It is probably because the adsorbent became saturated during the adsorption process.

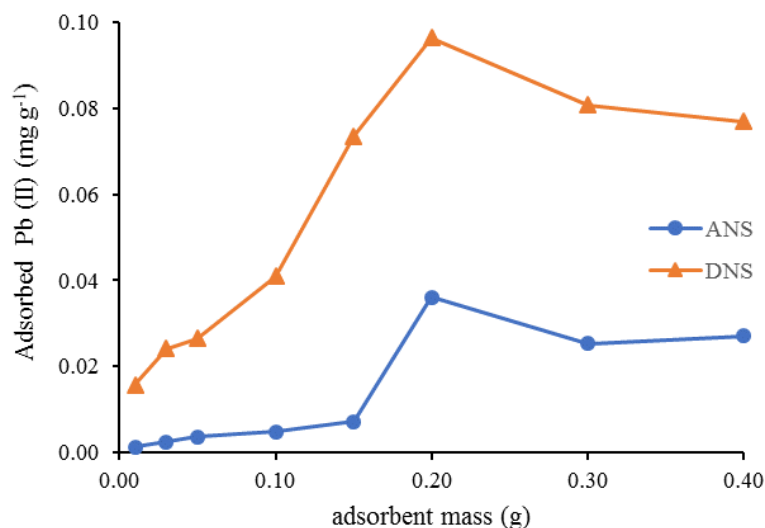


Figure 4. The impact of adsorbent dose

3.6 The adsorption kinetics of lead (II) ion

Lead (II) ion equilibrium on both adsorbents was obtained after 60 minutes of contact. Figure 5 depicts the influence of interaction time on lead ion adsorption. It is obvious that the adsorption increases until equilibrium is established as the contact time increases.

Table 4. The kinetics of lead (II) adsorption on ANS and DNS

Kinetic order models	R ²	
	ANS	DNS
zero	0.5436	0.4324
1st	0.5353	0.4186
2nd	0.4013	0.5176
3rd	0.4919	0.3825
Pseudo-1st	0.4773	0.3758
Pseudo-2nd	0.9915	0.9954

It is due to the presence of unoccupied spots on the surface of the slag. Pb (II) ion can no longer occupy the active sites of adsorbents after equilibrium is reached. Inferred from Figure 5, the amount of lead ion adsorbed by DNS is usually somewhat more than that of ANS. The outcome was enhanced as a result of the increased contribution of dithizone's active sites, such as the-NH and-SH groups. Several kinetic models have been fitted to the data gathered from this experiment. The various forms of kinetic reaction orders are summarized in table 4.

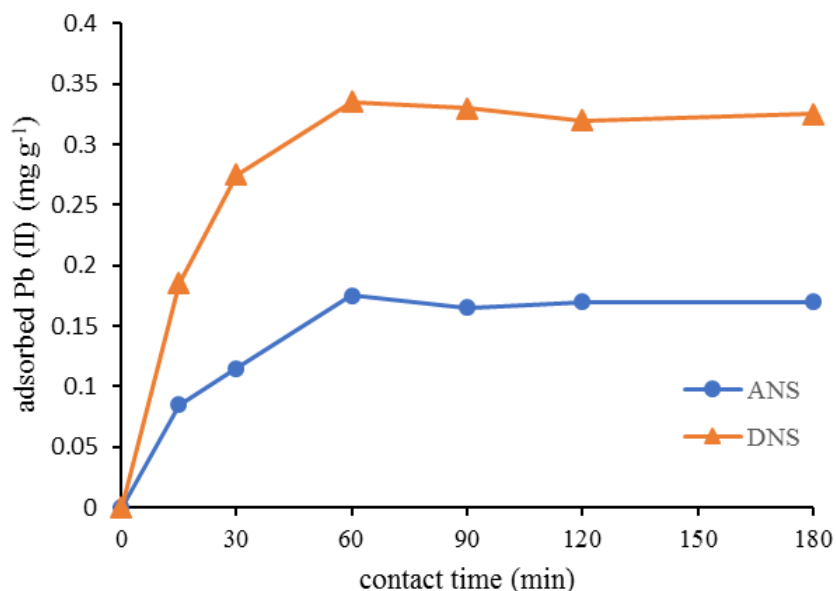


Figure 5. The impact of interaction time on the adsorption

Table 5. The value kinetic parameters

Adsorbent	Kinetic parameter of adsorption		
	*Adsorption rate constant, k_2 ($\text{g mg}^{-1} \text{min}^{-1}$)	Equilibrium concentration, q_e (mg g^{-1})	R^2
DNS	0.4213	0.3423	0.9954
ANS	0.3873	0.1869	0.9915

*Pseudo-second order kinetic

In accordance with table 4, Pb (II) ions were adsorbed according to pseudo-second-order kinetic models [26], with an R^2 value of more than 0.9. The resulting parameters, adsorption rate constant (k_2) and equilibrium adsorption capacity of slag (q_e), are shown in Table 5. According to the findings in Table 5, the adsorption rate of pseudo-second order (k_2) of DNS is larger than that of ANS for Pb (II), with 0.4213 and 0.3873 $\text{g mg}^{-1} \text{min}^{-1}$. In addition, the corresponding adsorption capacities (q_e) were 0.3423 and 0.1869 mg g^{-1} . According to table 5, the process of lead ion adsorption on the DNS is swifter and has a better adsorption capacity than on the ANS. The increase in adsorption rate is able to be attributable to the presence of extra active sites, such as NH and SH groups derived from dithizone.

3.7 The isotherm adsorption of lead (II) ion

The isotherm adsorption of lead (II) ion by DNS and ANS was investigated by performing adsorption experiments at varying initial lead concentrations and comparing the findings with the Freundlich and Langmuir isotherm models. Figure 6 depicts the impact of initial Pb (II) concentration

on DNS and ANS. The quantity of lead adsorbed by DNS rises from 10 to 80 mg L⁻¹ of initial concentration, showing that the accessible active sites of DNS have not been filled by lead ions. When the starting concentration is greater than 80 mg L⁻¹, however, the adsorbent cannot be enhanced since its surface may be completely occupied by Pb (II).

Table 6. Lead adsorption isotherm linearity value (II)

Adsorbent	R ²	
	Langmuir	Freundlich
DNS	0.9769	0.8695
ANS	0.8906	0.8373

Table 6 displays the findings of determining isotherm adsorption parameters using Freundlich and Langmuir models. The R² score in table 6 confirms that the Langmuir isotherm model is preferable to the Freundlich isotherm model. This model of isotherm adsorption is used to calculate q_{max} (adsorption capacity), K_L (Langmuir isotherm constant), and energy of adsorption (E_{ads}). Table 7 summarizes the results of parameter evaluation for the Langmuir isotherm model.

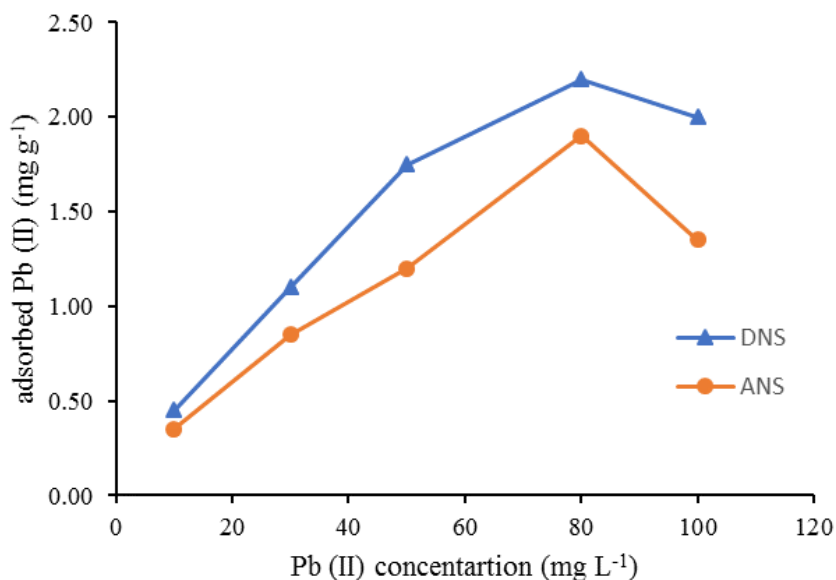


Figure 6. The impact of lead concentration on the adsorption

It is obviously seen from table 7 that DNS has a significantly larger maximum adsorption capacity and equilibrium constant than ANS. This is a direct result of the dithizone's extra SH and NH active groups. The energy absorption values for both DNS and ANS are greater than 20.920 kJ mol⁻¹. It suggests that Pb (II) adsorption by DNS and ANS is chemisorption. Adsorption has been divided into chemisorption and physisorption by Adamson and Gast [27]. Chemisorption happens when the E_{ads} is greater than 20.920 kJ mol⁻¹, whereas physisorption occurs when it is less.

Table 7. The linearity value of isotherm models for the adsorption of lead

Adsorbent	Parameter of Langmuir isotherm		
	q _{max} (mg g ⁻¹)	K _L (g L ⁻¹)	E _{ads} (kJ mol ⁻¹)
DNS	2.3753	0.1303	53.47
ANS	1.7307	0.0855	53.72

Conclusion

The loading of dithizone on nickel slag was accomplished satisfactorily. The adsorption capacity of nickel slag in adsorbing lead ion is greatly improved by loading dithizone onto the surface of nickel slag. Lead (II) adsorption is consistent with the pseudo-second order kinetic model and Langmuir isotherm.

References

- [1] W.E.M. L.B. Khalil, M.W. Rophael, The removal of the toxic Hg(II) salts from water by photocatalysis, *Appl. Catal. B Env.* 36 (2002) 125–130. [https://doi.org/10.1016/S0926-3373\(01\)00285-5](https://doi.org/10.1016/S0926-3373(01)00285-5).
- [2] M.E. Argun, S. Dursun, M. Karatas, M. Gürü, Activation of pine cone using Fenton oxidation for Cd(II) and Pb(II) removal, *Bioresour. Technol.* 99 (2008) 8691–8698. <https://doi.org/10.1016/j.biortech.2008.04.014>.
- [3] T.K. Naiya, A.K. Bhattacharya, S. Mandal, S.K. Das, The sorption of lead(II) ions on rice husk ash, *J. Hazard. Mater.* 163 (2009) 1254–1264. <https://doi.org/10.1016/j.jhazmat.2008.07.119>.
- [4] Z.H. Huang, F. Zhang, M.X. Wang, R. Lv, F. Kang, Growth of carbon nanotubes on low-cost bamboo charcoal for Pb(II) removal from aqueous solution, *Chem. Eng. J.* 184 (2012) 193–197. <https://doi.org/10.1016/j.cej.2012.01.029>.
- [5] M. Mudasir, R.A. Baskara, A. Suratman, K.S. Yunita, R. Perdana, W. Puspitasari, Simultaneous Adsorption of Zn(II) and Hg(II) Ions on Selective Adsorbent of Dithizone-Immobilized Bentonite in the Presence of Mg(II) Ion, *J. Environ. Chem. Eng.* 8 (2020) 104002. <https://doi.org/10.1016/j.jece.2020.104002>.
- [6] I. Mihailova, S. Dimitrova, D. Mehandjiev, Effect of the thermal treatment on the Pb (II) adsorption ability of blast furnace slag, *J. Chem. Technol. Metall.* 48 (2013) 72–79.
- [7] H. Shirzadi, A. Nezamzadeh-Ejhieh, An efficient modified zeolite for simultaneous removal of Pb(II) and Hg(II) from aqueous solution, *J. Mol. Liq.* 230 (2017) 221–229. <https://doi.org/10.1016/j.molliq.2017.01.029>.
- [8] D. Mudasir, D. Maryanti, G. Pramiyanti, G. Roto, Pre-concentration Study of Pb(II) and Cd(II) from Aqueous Solution Using Silica Gel Loaded with Dithizone, *J. Ion Exch.* 18 (2007) 516–517. <https://doi.org/10.5182/jaie.18.516>.
- [9] T. Pambudi, E.T. Wahyuni, M. Mudasir, Recoverable Adsorbent of Natural Zeolite / Fe₃O₄ for Removal of Pb (II) in Water, *J. Mater. Environ. Sci.* 11 (2020) 69–78.
- [10] M. Mudasir, K. Karelius, N.H. Aprilita, E.T. Wahyuni, Adsorption of mercury(II) on dithizone-immobilized natural zeolite, *J. Environ. Chem. Eng.* 4 (2016) 1839–1849. <https://doi.org/10.1016/j.jece.2016.03.016>.
- [11] Y. Zhang, C. Zhang, X. Zhang, L. Feng, Y. Li, Q. Zhou, Waste activated sludge hydrolysis and acidification: A comparison between sodium hydroxide and steel slag addition, *J. Environ. Sci. (China)*. 48 (2016) 200–208. <https://doi.org/10.1016/j.jes.2016.02.010>.
- [12] H. Gao, Z. Song, W. Zhang, X. Yang, X. Wang, D. Wang, Synthesis of highly effective absorbents with waste quenching blast furnace slag to remove Methyl Orange from aqueous solution, *J. Environ. Sci.* 53 (2016) 68–77. <https://doi.org/10.1016/j.jes.2016.05.014>.
- [13] E.A. Oluwasola, M.R. Hainin, M.M.A. Aziz, Characteristics and utilization of steel slag in road construction, *J. Teknol.* 70 (2014) 117–123. <https://doi.org/10.11113/jt.v70.3591>.

- [14] S.M. Park, J.G. Jang, N.K. Lee, H.K. Lee, Physicochemical properties of binder gel in alkali-activated fly ash/slag exposed to high temperatures, *Cem. Concr. Res.* 89 (2016) 72–79. <https://doi.org/10.1016/j.cemconres.2016.08.004>.
- [15] A. Agarwal, N.K. Agrawal, V. Gupta, S. Giri, Removal of Pb & Ni from industrial wastewater by using brass industry waste (Slag) as an adsorbent, *Adv. Appl. Sci. Res.* 3 (2012) 2468–2473
- [16] D.H. Kim, M.C. Shin, H.D. Choi, C. Il Seo, K. Baek, Removal mechanisms of copper using steel-making slag: adsorption and precipitation, *Desalination.* 223 (2008) 283–289. <https://doi.org/10.1016/j.desal.2007.01.226>.
- [17] A. Agarwal, M. Saxena, M. Agarwal, Removal of Pb & Cr from their aqueous solution by using brass industry waste (Slag) as an adsorbent, *Int. J. Environ. Sci.* 3 (2013) 1931–1937. <https://doi.org/10.6088/ijes.2013030600015>.
- [18] X. Chen, W.H. Hou, G.L. Song, Q.H. Wang, Adsorption of Cu, Cd, Zn and Pb ions from aqueous solutions by electric arc furnace slag and the effects of pH and grain size, *Chem. Biochem. Eng. Q.* 25 (2011) 105–114.
- [19] J. Duan, B. Su, Removal characteristics of Cd(II) from acidic aqueous solution by modified steel-making slag, *Chem. Eng. J.* 246 (2014) 160–167. <https://doi.org/10.1016/j.cej.2014.02.056>.
- [20] B.N. Huda, E.T. Wahyuni, M. Mudasir, Eco-friendly immobilization of dithizone on coal bottom ash for the adsorption of lead(II) ion from water, *Results Eng.* 10 (2021) 100221. <https://doi.org/10.1016/j.rineng.2021.100221>.
- [21] Mudasir, D. Siswanta, P.D. Ola, Adsorption Characteristics of Pb(II) and Cd(II) Ions on Dithizone-loaded Natural Zeolite, *J. Ion Exch.* 18 (2007) 564–569. <https://doi.org/10.5182/jaie.18.564>.
- [22] L. Liang, Y. Yan, Application of Modified Nickel Slag Adsorbent on the Removal of Pb²⁺ and Cu²⁺ from Aqueous Solution, *Chinese J. Struct. Chem.* 35 (2016) 879–888. <https://doi.org/10.14102/j.cnki.0254-5861.2011-1002>.
- [23] A.M.M.Z. Yudiarto, Synthesis of Magnesium Oxide from Ferronickel Smelting Slag Through Hydrochloric Acid Leaching-Precipitation and Calcination, in: *Miner. Met. Mater. Soc.*, 2017: pp. 247–258. <https://doi.org/10.1007/978-3-319-52192-324>
- [24] R.B. Downs, Bob;Swaminathan, *American Mineralogist*, 1993.
- [25] R.G. Pearson, Hard and soft Acids and Bases, HSAB, Part I, *J. Chem. Educ.* 45 (1968) 581–587
- [26] Y.S. Ho, G. McKay, Pseudo-second order model for sorption processes, *Process Biochem.* 34 (1999) 451–465. [https://doi.org/10.1016/S0032-9592\(98\)00112-5](https://doi.org/10.1016/S0032-9592(98)00112-5)
- [27] A.W. Adamson, *Physical Chemistry of Surface*, 5th ed., John Wiley and Son Inc., New York, 1990

(2022); <http://www.jmaterenviromsci.com>